DOE/NASA/0011-1
NASA CR-168153

NASA-CR-168153
19830016586

Classification of Journal Surfaces Using Surface Topography Parameters and Software Methods to Compensate for Stylus Geometry

Cheng-Jih Li, Warren R DeVries,
and Kenneth C Ludema
University of Michigan

April 1983

NF02595

Prepared for
NATIONAL AERONAUTICS AND SPACE ADMINISTRATION
Lewis Research Center
Under Cooperative Agreement NCC 3-11

for
U.S. DEPARTMENT OF ENERGY
Conservation and Renewable Energy
Office of Vehicle and Engine R&D

Printed in the United States of America

Available from
National Technical Information Service
U S Department of Commerce
5285 Port Royal Road
Springfield, VA 22161

NTIS price codes[1]
Printed copy A04
Microfiche copy A01

[1]Codes are used for pricing all publications The code is determined by the number of pages in the publication Information pertaining to the pricing codes can be found in the current issues of the following publications, which are generally available in most libraries *Energy Research Abstracts (ERA), Government Reports Announcements* and Index (*GRA* and I), *Scientific and Technical Abstract Reports (STAR),* and publication, NTIS-PR-360 available from NTIS at the above address

DOE/NASA/0011-1
NASA CR-168153

Classification of Journal Surfaces Using Surface Topography Parameters and Software Methods to Compensate for Stylus Geometry

Cheng-Jih Li, Warren R DeVries,
and Kenneth C Ludema
University of Michigan
Ann Arbor, Michigan 48109

April 1983

Prepared for
National Aeronautics and Space Administration
Lewis Research Center
Cleveland, Ohio 44135
Under Cooperative Agreement NCC 3-11

for
U S DEPARTMENT OF ENERGY
Conservation and Renewable Energy
Office of Vehicle and Engine R&D
Washington, D C 20545
Under Interagency Agreement DE-AI01-80CS50194

CLASSIFICATION OF JOURNAL SURFACES USING SURFACE TOPOGRAPHY PARAMETERS AND SOFTWARE METHODS TO COMPENSATE FOR STYLUS GEOMETRY

Chen-Jih Li, Warren R. DeVries,
and Kenneth C. Ludema
University of Michigan
Ann Arbor, Michigan

SUMMARY

This report deals with the statistical characteristics of surface profiles measured with a stylus tracer; there definitions, an application and enhancement using software to compensate for stylus geometry effects. After defining some of the common height sensitive profile statistics, they are used classify the journal surfaces of diesel engine crank shafts produce by manufacturing methods that yield significantly different service life.

Software methods are presented to try to reconstruct a surface profile from discrete measurements by accounting for the finite radius of the stylus tracer.

Results indicate that using three parameters: RMS roughness, skewness and kurtosis, and a classification method termed "separated subspaces", the journal surfaces produced by different combinations of grinding and lapping can be classified. The work on compensating for stylus geometry, which is verified using both mathematical simulation and experimental measurements, indicates that, at least for simple profile geometries compensation for stylus radius' can reduce errors to less than .4%.

1. INTRODUCTION

Before 1950 surfaces were generated and refined exclusively by traditional mechanical methods (e.g. cutting, grinding, honing, lapping and polishing). The need to machine the high temperature alloys used in jet engines stimulated the development of many additional material removal techniques. These nontraditional methods include electrochemical cutting and grinding, spark discharge machining, electron beam, ion beam, laser and plasma arc removal techniques [1]. Thus in the early stages, finish was specified by the process, but with these non-traditional methods as the driving force, more quantitative methods of specification were needed.

At the submicroscopic level most surfaces are far from smooth and plane, they have the characteristics of a range of mountains with peaks and valleys. A number of causes contribute to the roughness. First is the mark left by the tool or grit itself, which will be of a periodic nature for cutting process and more random for abrasive or nontraditional processing methods. Second there is a finer structure due to tearing of the metal during machining, the debris of the built-up edge and the small irregularities in the shape at the tip of the tool. Finally, especially in alloy steels there may be microscopic cracks at grain boundaries [2]. Thus the resulting surface is a function of the process used, the conditions at the cutting edge and the material being processed.

These characteristics of surface roughness are very important in many respects from both a scientific and industrial point of view. Particularly in contact problems that involve wear, lubrication, heat transfer and sealing, surface roughness plays a role [3-12]. For example, in forced convection heat transfer, it is well known that the heat transfer rate can be enhanced through proper changes of surface roughness [8]. Also the rate of fouling or the deposition of scale on the surfaces affects the useful life of the heat transfer equipment significantly [7]. A large number of engineering components and devices are directly dependent upon surface characteristics for their performance. These include both sliding and rolling bearings of all types, seals, brakes, clutches, joints, springs, fasteners, cams, splines and gears, particularly if the requirements of interchangeability of machine elements considering the fits, wear, lubrication, etc., that are involved [13].

For some of these applications there is an optimum surface. For instance, the cylinder walls of an internal combustion engine may be too smooth to allow rapid spreading and wetting by oil or too rough to enable the surface asperities to support the applied loads without galling [13]. The topic of quantitatively expressing the extent of roughness of the surface is really worthy of careful study. Specifically, it would be desirable to characterize the form of a surface, be able to quantitatively relate this form to the function of the surface, and then to know exactly what processes can be used to generate this form.

The ways of measurement of the surface profiles can be categorized as follows:

a. Non-Contact Profile Measurement Methods [14]:

One example is optical methods, which allow the specimen to be investigated without destroying it or subjecting it to a strain or wear. Other methods that have been used involve capacitance or pneumatics as the measurement principle.

b. Contact Profile Measurement Methods:

Instruments with stylus tracers in mechanical contact with the surface are the most common way of measuring surface topography. Stylus methods have a shortcoming in that there exists an error from the influence of stylus geometry, but it does provide an immediate numerical characterization of a surface, so it is used widely in industry, is the most direct measurement of geometry and is used in U.S. Standards [15].

Statistical considerations are intimately tied up with the measurment of surfaces. Statistical parameters are used to characterize different surfaces with the expectation that there will be little variation in these parameters over the surface [16]. Various modifications and improved surface finish parameters have been proposed by Reason [17], Pesante [18], Ehrenreich [19], Teague [20] and others.

This report concentrates on measurements made with stylus devices that are digitized representations of a stylus trace. As a starting point, some of the common parameters used to characterize the form of a profile trace are defined. This is followed by an application of these parameters to the problem of characterizing the journal surfaces of crank shafts that are produced by different manufacturing methods and have vastly different life in service. The final piece of work develops new methods for deconvolving or compensating for the effects of stylus geometry on the measurements made with a tracer.

II. STATISTICAL CONCEPTS FOR DESCRIBING TYPICAL SURFACE TOPOGRAPHY PARAMETERS

The most common surface finish measurement variable is roughness height, which is the numerical value of the average distance, in micro-inches or microns, of each point on the surface profile from a defined line called the reference center line. Once this reference center line is set, each roughness height measurement, Y_i for $i = 1,\ldots,N$, of the surface are referenced normal to this line. All computations of the characteristics of the profile are based on the measured roughness height. Obviously it is essential to define a reference center line properly.

There are several methods that have been used in defining the reference center line [21,22], they are:

a. Envelope Method (E - System):

Imagine that there is a large circle (often 25 mm in diameter) rolling over a surface, and regard the locus of the center of this circle as the reference center line. This method is used in some European countries.

b. Ten Point Average Method:

This method requires finding the 5 highest peaks and 5 lowest valleys of the profile, and calculating the average value of these ten points. This average value is regarded as the reference center line.

c. Mean Line Method:

The mean line is selected so that on each side of it the areas enclosed by the profile are equal, i.e. the centroid of the profile. For discrete profiles, the area for each profile is assumed to be a rectangle of height y_i and with a constant width Δx. It turns out that we can use an alternative definition for easy computation which takes the reference center line as a line parallel to the general direction of the profile such that the average height of the profile on one side of it is equal to the average height on the other side. With the previous assumptions, the mean line in this case is simply the average, i.e. if the height of the point at x_i is Y_i, the mean can be mathematically expressed as:

$$\bar{Y} = \frac{1}{N} \sum_{i=1}^{N} Y_i \qquad (1)$$

This method is the standard in U.S., Canada and Britain.

d. Least Squares Line Method:

The well known formulas for linear regression are used to get the least square line, which is regarded as the reference center line. With this method the reference line is a function of position as given by:

$$\bar{Y}_i = a + bx_i \qquad (2)$$

where

a = the intercept of the least square line with the y axis, and

b = the slope of the least square line (3)

In practice, the Envelope Method is not used very often because of the difficulty of determining the locus. The Ten Point Average Line Method leads to a reference center line below the major surface features for deeply pitted surfaces. As a result it is common that people often use the Mean Line Method and the Least Square Line Method.

The Mean Line Method gives a "horizontal" reference line which cannot compensate for the "tilt" in the profile, whereas the Least Square Line Method does compensate for tilt in the experimental setup.

Now, let us have a brief survey of the statistics which are most commonly used to represent the properties of a measured surface. All of these parameters are based on a profile like that shown in Fig. (1a). They refer to deviations from a reference line based on one of the methods previously described. Therefore, all computations are made using:

$$y_i = Y_i - \bar{Y} \tag{4}$$

where $\bar{Y}$ is the reference line, Y_i is a measured value and y_i is the deviation from the reference. This transformation leads to another discrete profile which may be interpreted as shifting the measured profile to a zero mean level, as shown in Fig. (1b).

HEIGHT PARAMETERS:

Measures of dispersion show the degree of spread of the data around the central value. The most common one is standard deviation, or RMS roughness. Based on deviations from the mean given by Eq. (4), the RMS roughness

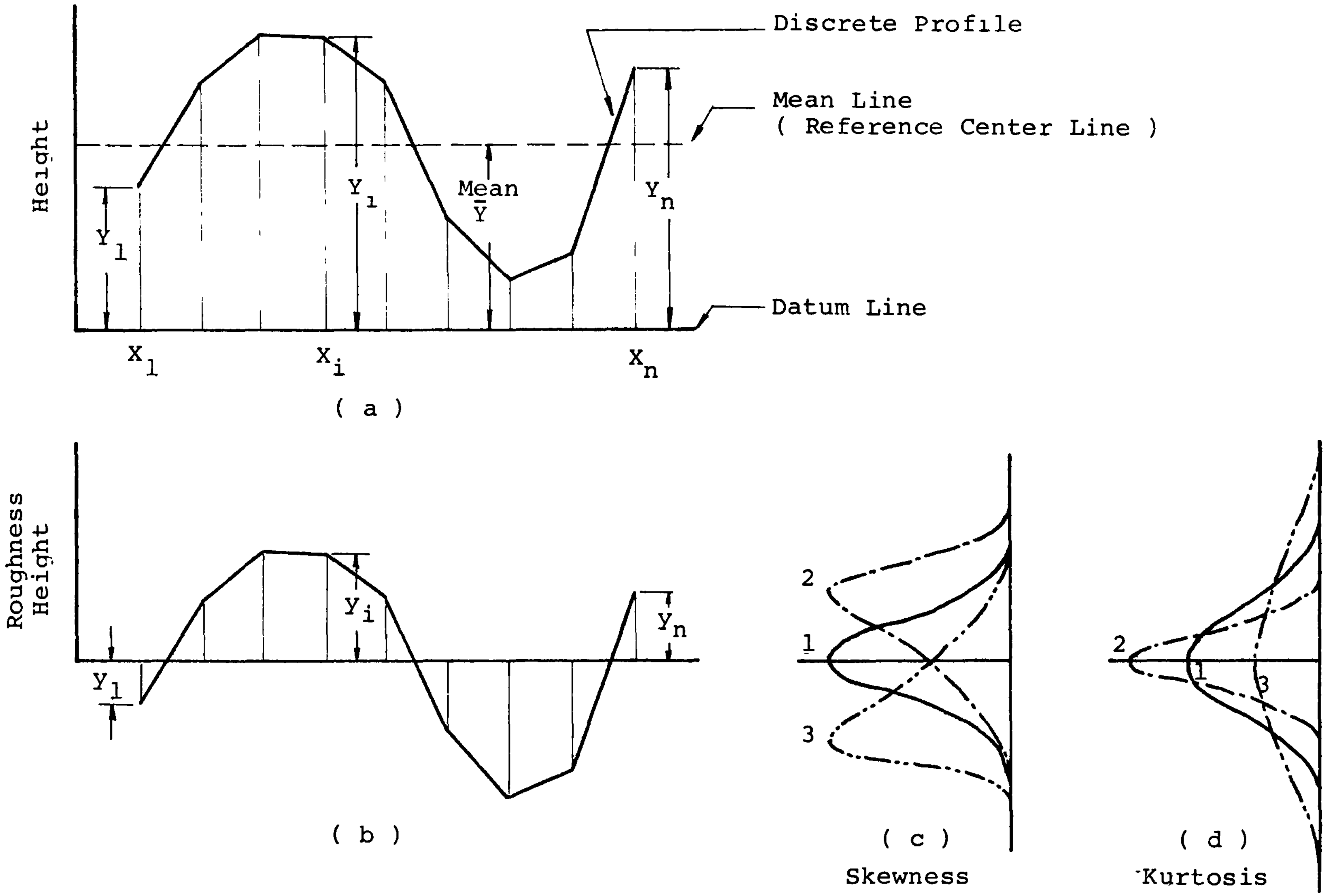

Figure 1. Schematically illustrating the statistical parameters.

is defined as:

$$R_q = \sqrt{\frac{1}{N} \sum_{i=1}^{N} y_i^2} \quad (5)$$

Today, because of its greater simplicity, arithmetic averaging is much more commonly used, and is, in fact, the American Standard for roughness. Arithmetic average (AA) roughness is defined as:

$$R_a = \frac{1}{N} \sum_{i=1}^{N} |y_i| \quad (6)$$

HEIGHT DISTRIBUTION PARAMETERS:

There are two parameters which were proposed by Al-Salihi [23] to describe height distribution, they are skewness and kurtosis. While they are used in characterization of surface profiles, they are well known descriptors of statistical distributions.

Skewness means lack of symmetry, and measures of skewness show the extent to which the distribution departs from symmetry. Skewness is defined as:

$$\gamma_1 = \frac{1}{N} \sum_{i=1}^{N} \left(\frac{y_i}{R_q}\right)^3 \quad (7)$$

Refer to Fig. (1c). If $\gamma_1 = 0$, the distribution is symmetric, such as a Gaussian distribution, shown as curve 1. If $\gamma_1 > 0$, the distribution is skewed to a higher level as shown by curve 2. Whereas, if $\gamma_1 < 0$, the distribution is skewed to a lower level as shown in curve 3. The positive skewed surfaces ($\gamma_1 > 0$) is thought to be more suitable for load carrying than surfaces negatively skewed.

Kurtosis may be defined as "peakness". A measure of kurtosis serves to differentiate between a flat distribution curve and a sharply peaked curve. In other words, it enables the squareness of the profile to be described. Kurtosis is defined as:

$$\gamma_2 = \frac{1}{N} \sum_{i=1}^{N} \left(\frac{y_i}{R_q}\right)^4 \qquad (8)$$

For a Gaussian distribution, γ_2 is equal to 3, which is shown as curve 1 in Fig. (1d). If $\gamma_2 > 3$, the distribution is more sharply peaked than Gaussian as shown in curve 2, and is defined as leptokurtic. If $\gamma_2 < 3$, the distribution is flatter than Gaussian as shown in curve 3 and is defined as platykurtic.

LENGTH SENSITIVE PARAMETERS:

One parameter in this group is the autocorrelation function, which was first noticed by Wormersley and Hopkins [24] as a time series. However it was Peklenik [25] who first applied it to classification.

The autocorrelation gives an estimate of the relation between y_i and y_{i-k}, which are the values of y_i at horizontal intervals of length, $k(\Delta x)$. Autocorrelation is defined as:

$$\hat{\rho}_k = \frac{\sum_{i=k+1}^{N} y_i y_{i-k}}{\sum_{i=1}^{N} y_i^2} \qquad (9)$$

In addition to the autocorrelation, the spectrum, which is the Fourier transform of the autocorrelation, is often used. Often the spectrum is most effective when dealing with highly periodic profiles.

III. HOW MEASUREMENTS ARE MADE

The procedure used to make profile measurements involves digitizing the analog stylus deflections, and storing this data. The setup used is typical of many laboratory installations, this one using a Bendix Proficorder and a Digital Equipment Corporation (DEC) LSI-11/2 microcomputer.

Figure (2) shows the stylus transducer setup that is used to convert the vertical motion of the diamond stylus, with radius r, to an analog voltage. The lever arrangement causes the core of a linear variable differential transformer (LVDT), to move. The resulting A.C. signal is demodulated to provide a D.C. voltage proportional to the deflection of the stylus tip.

The stylus traverses at a linear velocity V, which is assumed to be constant. To assure a straight path for this motion, the stylus is referenced to an optical flat. However, this straight path does not assure that the stylus has a path parallel to the surface being measured, so that it is possible to have a "tilt" in the measured profile.

The data acquisition setup is shown in Fig. (3), and is designed to provide an analog trace of the surface, as well as a digitized trace. A Brush recorder is used to indicate the analog trace on one channel, with the signal coming directly from the tracer amplifier. Between the amplifier and the analog to digital converter (ADC) on the microcomputer, an active low pass filter is installed to avoid aliasing as explained below.

The aliasing problem can best be explained in terms of the sampling interval, Δx. If we sample at points which are too

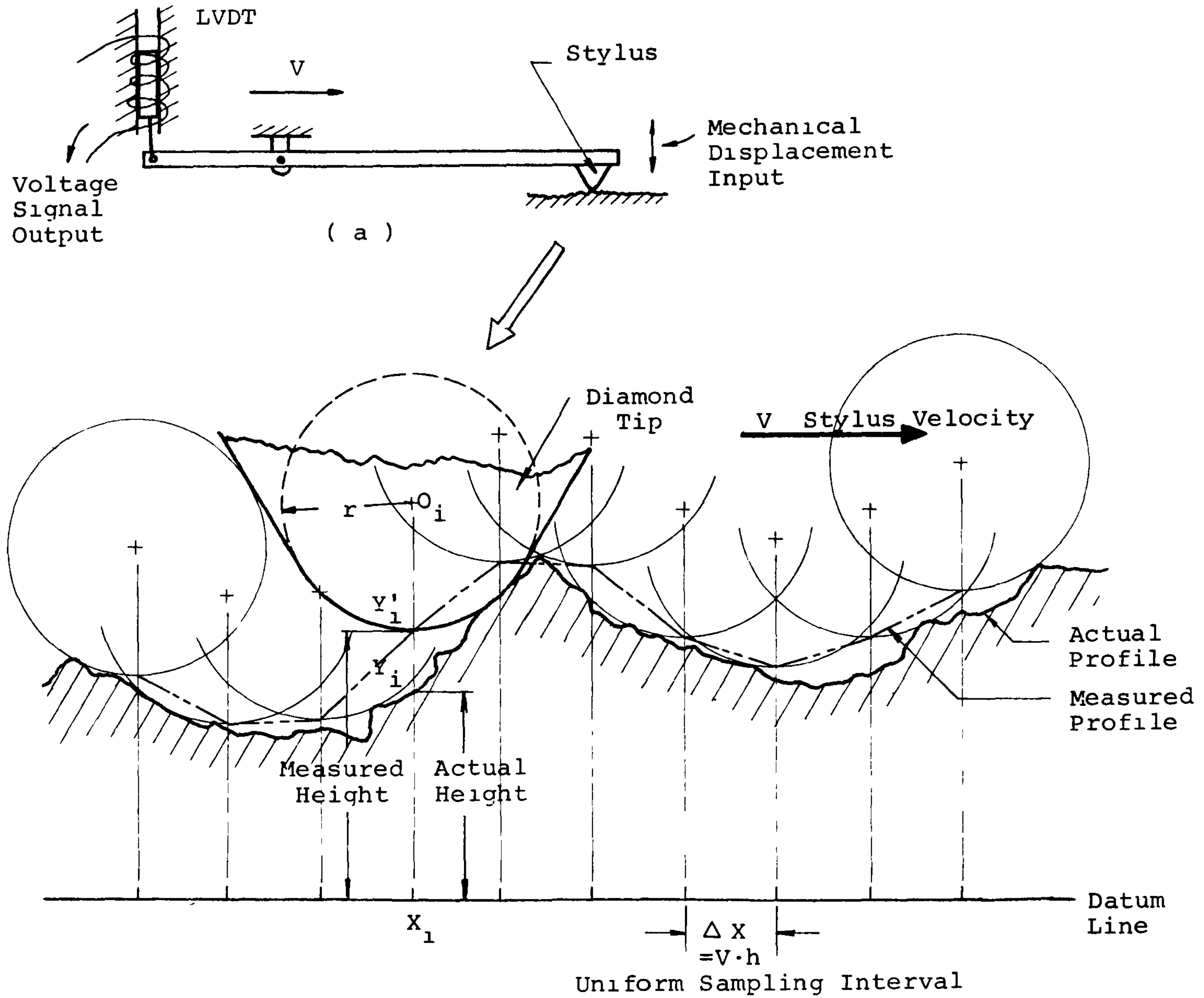

Figure 2. Schematically illustrating the (a) linear variable differential transformer, (b) locus of stylus tip when measuring.

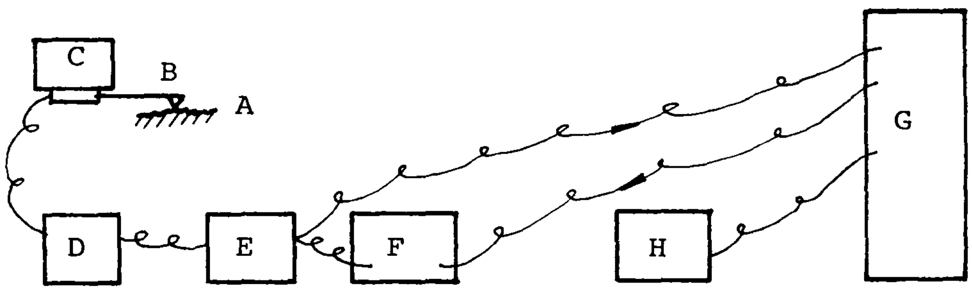

A -- Journal Specimen
B -- Stylus
C -- Linear Variable Differential Transformer
D -- Amplifier
E -- Filter
F -- Recorder
G -- LSI-11/2 Microcomputer
H -- CRT

Figure 3. Schematically illustrating the set-up.

close together, it will yield correlated and highly redundant data, and thus unnecessarily increase the labor and cost of calculations. On the other hand, sampling at points which are too far apart will lead to confusion between the low and high frequency components in the original data. This later problem is called aliasing.

Consider a continuous record which is uniformly sampled with h seconds time interval, i.e. a sampling rate of 1/h samples per second. If the velocity of stylus motion is V, the sampling interval will be $\Delta x = V \cdot h$, refer to Fig. (2). However, we need at least two samples per cycle to define a frequency component in the original data. Hence, the highest frequency which can be defined by sampling at a rate of 1/h samples per second is 1/2h Hz. Frequencies in the original data above 1/2h Hz will be folded back into the frequency range from 0 to 1/2h Hz, and be confused with data in this lower range. This cutoff frequency is called the Nyquist frequency. To be on the safe side the filter break frequency is set at 1/3h.

The digitized signal is sent back to the second channel of the Brush recorder using a digital to analog converter (DAC) so that it can be visually compared with the incoming analog signal. For subsequent analysis, the digitized data is also stored on a floppy disk.

Once the data on a profile has been acquired, it is conditioned as follows. The trend is defined as any frequency component whose period is longer than the record length. This type of component cannot be removed by highpass digital filtering as will be mentioned later. Here we chose the least squares procedures, Eqs. (2) and (3), to remove the linear trend, which usually arises from "tilt" or lack of parallelism between the optical flat and surface being measured.

To remove waviness often associated with errors of form, highpass filtering, like that often done with wavelength cutoff analog circuitry, is used. This can be done by fast Fourier transform because only a finite range Fourier series or transform can actually be computed with digitized data, and this finite range can always be considered as the period of an associated Fourier series. Digital filtering methods are used to filter out the lower frequencies, (long wavelength waviness) of the profile by choosing a wavelength cutoff.

Once this is done, the profile statistics described in Section II can be computed.

IV. AN APPLICATION OF SURFACE STATISTICS TO CLASSIFICATION OF JOURNAL SURFACES ON CRANK SHAFTS

The normal finishing steps on journal surfaces involves grinding and lapping. The relative direction of these two operations is felt to be critical. For example, if the crank will rotate clockwise, then the grinding should be done counter-clockwise followed by lapping in a clockwise direction. One can speculate that this order could tend to minimize the directional tendency of asperity tips, i.e. the grinding may give the asperities a direction and if lapping works on the tip of the asperity it will flatten the asperity and shift material in the opposite direction. It is said that there is quite a difference in bearing life when using the journal bearings made through different manufacturing methods. For example, the life of the journals which are ground and lapped in the same direction is 500 working hours, whereas the life of those which are ground and lapped in the opposite direction is about 5000 working hours. The effect of the finishing steps is so great as to be worthy of studying.

An experiment was made by applying the previous ideas on the measurement of surface profiles to several journal surfaces of diesel engine crank shafts. An additional purpose was to determine if there is a parameter or several parameters that can be used to classify the journal surfaces according to their manufacturing steps and the relative directions of grinding and lapping.

SAMPLE SPECIMENS:

Coupons to be measured were cut out of the journal surfaces of new engine crankshafts, some from the main bearing surfaces and others from the connecting rod throw. Figure (4), illustrates where the various samples are located on a typical crank originally.

Three sets of specimens, from three cranks, were made available: ground only and unlapped (U), ground and lapped in the same direction as grinding (LSD), and ground and lapped in the direction opposite to grinding (LOD). Table 1 groups the samples according to their manufacturing procedure.

MEASURING:

The set up of this experiment is the same as shown schematically in Fig. (3). Surface profile traces were made using a Bendix Proficorder equipped with a stylus having a 12.7 μm radius. The analog output of the stylus displacement was digitized, bypassing the analog filters used for setting the wavelength cutoff. A Krohn-Hite 3323 active filter acted as an anti-aliasing filter. Based on the traverse speed of the stylus, .3175 mm/s, and selection of a spatial sample interval, ΔX = .005 mm, the temporal rate is determined and the break frequency for the antialiasing filter was selected on the conservative side to be one third the sampling frequency.

Using the conditions mentioned above, 4 longitudinal traces were made at different positions on each journal coupon. In each case, 512 points were sampled in each trace, for a total stroke of slightly more than 2.5 mm.

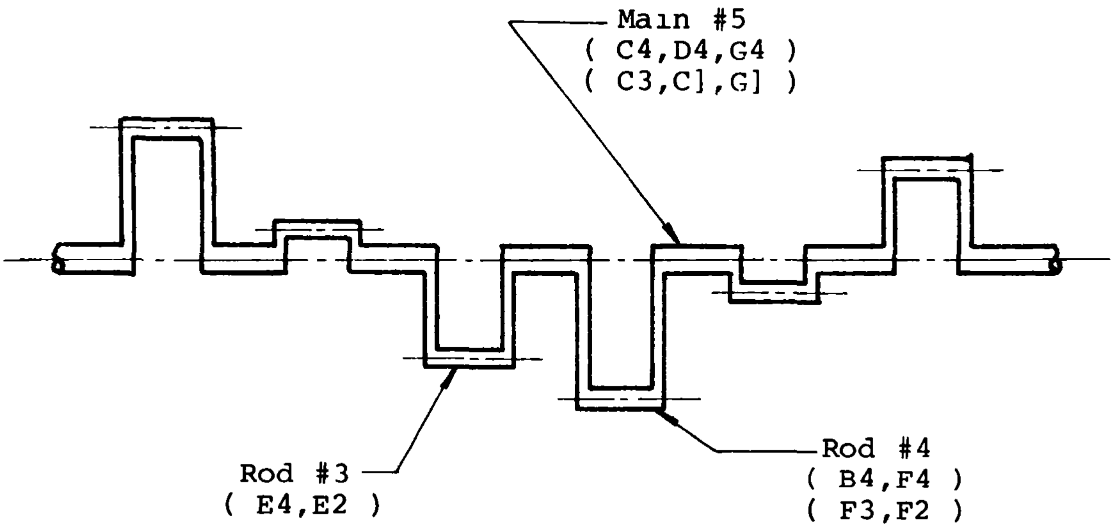

Figure 4. Schematically illustrating the location of the samples on a crankshaft.

Manufacturing Procedure	Specimen Identification
Ground only Unlapped (U)	B4,D4,E4,E2
Ground and Lapped in Same Direction (LSD)	C4,C3,C1
Ground and Lapped in Opposite Direction (LOD)	F4,G4,F3,G1,F2

Table 1. Group the samples according to their manufacturing procedures

These data were analyzed using the least squares reference line, Eq. (2), and the statistical parameters given by Eqs. (5) through (8) were computed. Reference [27] gives complete details on the computational methods used.

THE IDEA OF THE "RMS - SKEWNESS - KURTOSIS SPACE":

By comparing all the statistical parameters listed in Tables (2.1-2.3), it is true that the "ground only" specimen can be easily recognized from the other two kinds of specimen by just looking at the arithmetic averaging or RMS roughness. Owing to the similarity between arithmetic average and RMS, we choose only one of them, Rq, as a characteristic. The remaining parameters to describe the characteristics of the profile are Rq, skewness and kurtosis. Because every specimen has a set of values, we can regard it is a set of coordinates in a space constituted by these three characteristic axes. Since the values of coordinates are related to the wavelength we choose, we hope we can classify all the data points located in the defined space into three groups by choosing a suitable wavelength cutoff.

THREE MODELS OF CLASSIFICATION:

It is supposed that all the data points with the same manufacturing procedure will cluster into a sphere around a certain center. We took the average of all the data points with the same manufacturing method as the center of the sphere, shown in Table (3), and found that wavelength

Wavelength Cutoff	Group Type	ID	Ra	Rq	r_1	r_2
0.8 mm	U	B4	0.912	1.099	-0.266	2.836
		D4	0.579	0.719	-0.163	2.785
		E4	0.996	1.251	0.014	3.008
		E2	1.387	1.745	0.412	3.249
	LSD	C4	0.218	0.266	0.126	2.934
		C3	0.222	0.301	-0.828	8.132
		C1	0.283	0.365	-0.053	5.273
	LOD	F4	0.387	0.457	0.009	2.160
		G4	0.229	0.275	0.081	2.431
		F3	0.404	0.499	-0.334	3.428
		G1	0.330	0.447	-0.610	4.359
		F2	0.411	0.538	0.445	4.008

Table 2.1 Statistical parameters for 0.8 um wavelength cutoff (each parameters got from the average of 4 traces)

Wavelength Cutoff	Group Type	ID	Ra	Rq	γ_1	γ_2
0.25 mm	U	B4	0.579	0.755	-0.485	4.204
		D4	0.561	0.706	-0.234	3.044
		E4	0.877	1.103	-0.161	3.163
		E2	0.969	1.218	0.002	3.113
	LSD	C4	0.165	0.211	-0.140	3.745
		C3	0.134	0.188	-0.339	9.768
		C1	0.163	0.216	0.615	16.867
	LOD	F4	0.269	0.338	-0.033	3.140
		G4	0.154	0.199	0.260	3.734
		F3	0.315	0.405	-0.245	3.992
		G1	0.178	0.246	-0.408	6.222
		F2	0.278	0.388	0.138	4.893

Table 2.2 Statistical parameters for 0.25 mm wavelength cutoff (each parameters got from the average of 4 traces)

Wavelength Cutoff	Group Type	ID	Ra	Rq	γ_1	γ_2
0.08 mm	U	B4	0.441	0.570	-0.385	4.286
		D4	0.451	0.567	-0.169	2.945
		E4	0.738	0.934	-0.002	3.140
		E2	0.792	0.996	-0.096	3.074
	LSD	C4	0.084	0.106	-0.217	3.233
		C3	0.084	0.118	-0.377	8.774
		C1	0.096	0.134	0.690	23.461
	LOD	F4	0.135	0.175	-0.178	3.869
		G4	0.102	0.133	-0.125	4.249
		F3	0.175	0.233	-0.854	5.725
		G1	0.106	0.156	-0.231	11.198
		F2	0.147	0.200	-0.366	4.739

Table 2.3 Statistical parameters for 0.08 mm wavelength cutoff (each parameters got from the average of 4 traces)

Wavelength Cutoff (mm)	U	LSD	LOD
0.8	(1.204,-0.001, 2.970)	(0.311,-0.252, 5.446)	(0.443,-0.082, 3.277)
0.25	(0.946,-0.220, 3.381)	(0.205, 0.045,10.127)	(0.315, 0.058, 4.396)
0.08	(0.767,-0.163, 3.361)	(0.119, 0.032,11.823)	(0.179,-0.351, 8.028)

Table 3 Reference center points (Standard deviation, Skewness, Kurtosis)
(each value is the average of the same group)

cutoff did affect the position of this center. Thus we examined some models to find the best wavelength cutoff for clearly distinguishing the three conditions.

a. Totally Separate Sphere Range Model:

If we choose the distance between the farthest individual point and the corresponding center point as the radius and draw a sphere, we get three spheres with three different centers. The optimal condition for which we can distinguish these three spheres, which stand for three different ways to make journal bearing, is to maximize the distance between all the centers.

Since we have three centers, the distance between every pair of centers are listed in Table (4), the maximum radius each sphere may have can be considered as follows. Say we have three spheres with centers at points A,B,C, and the corresponding sides are a,b,c. If there is a smallest side, e.g. c, then both spheres, which have their center at either tip of side c, may have a maximum radius equal to c/2. The maximum radius of the third sphere is equal to the difference between the smaller side and c/2. This can be easily understood when we look at the triangle constituted of the three centers as shown in Fig. (5).

Following the previous idea, the procedure to do this is to find the three centers under different wavelength cutoffs. Then calculate the maximum radius

	Wavelength cutoff (mm)		
	0.8	0.25	0.08
U - LSD	9.599	10.361	10.831
LSD - LOD	3.058	5.837	5.424
LOD - U	7.652	6.960	7.733

Table 4 Distance between group centers

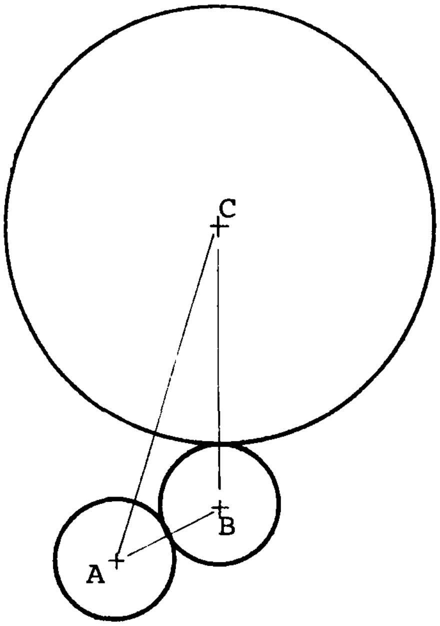

(a) 0.8 mm wavelength
cutoff

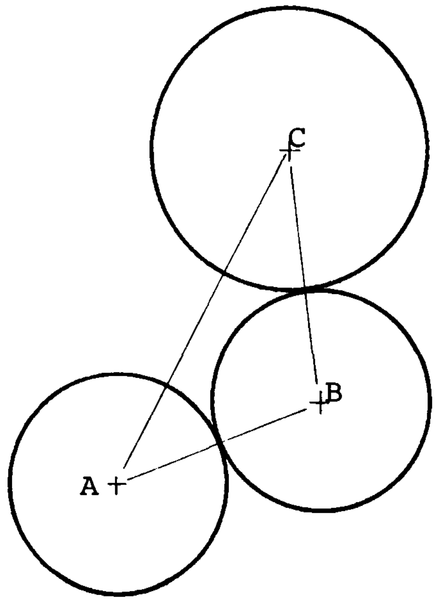

(b) 0.25 mm wavelength
cutoff

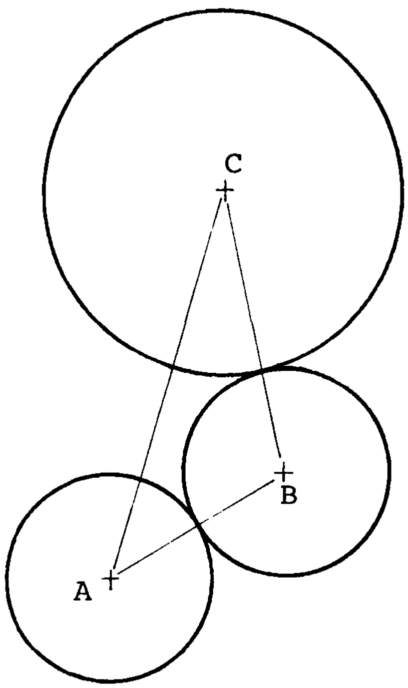

(c) 0.08 mm wavelength
cutoff

A -- Center Point of " U " Group

B -- Center Point of " LSD " Group

C -- Center Point of " LOD " Group

Figure 5. "Totally Separated Sphere Range" for three different wavelength cutoffs.

each sphere may have, and check the number of data points that fail to fall into the corresponding range. The wavelength cutoff which minimizes this failure is the one selected.

b. Minimized Overlapping Area Model:

This idea is somewhat similar to the previous one. The main difference is that we choose the longest distance between each data point and its corresponding center as radius of the sphere. We got three spheres from three cases. The wavelength cutoff we need is the one which produces minimum overlap of the three spheres, as shown in Fig. (6).

c. Separated Subspaces Model:

The third approach is based on the idea that if we find the three centers first, then the data points of the same group should have a shorter distance from the corresponding group center than those from the other two group centers. This can be expressed geometrically, refer to Fig. (7). Imagine a triangle with three centers A,B,C as its tips. The three planes which are perpendicular and bisect the three sides individually will intercept at a line called the centroid line. These three planes divide the space into three subspaces. The data points from the same group should fall into the same subspace. Since the distance between a data point and the center point in the same subspace will be the shortest one among

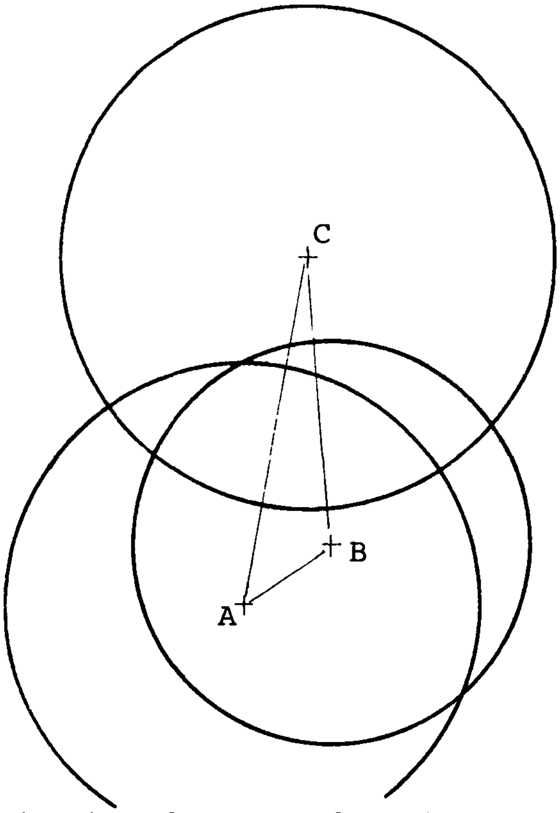

(a) 0.8 mm wavelength
cutoff

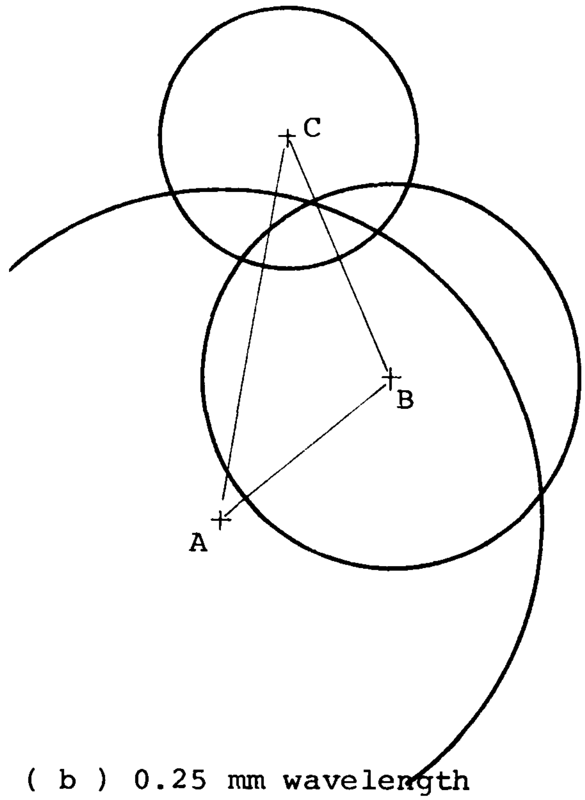

(b) 0.25 mm wavelength
cutoff

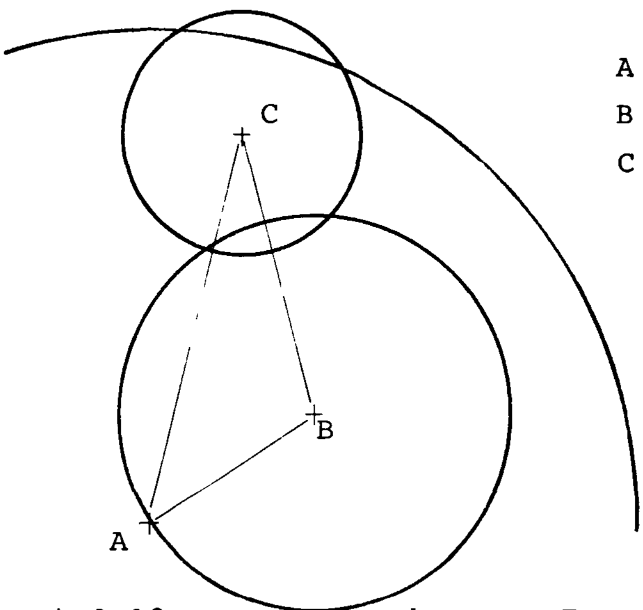

(c) 0.08 mm wavelength
cutoff

A -- Center Point of "U" Group

B -- Center Point of "LSD" Group

C -- Center Point of "LOD" Group

Figure 6. "Minimized Overlapping Area".

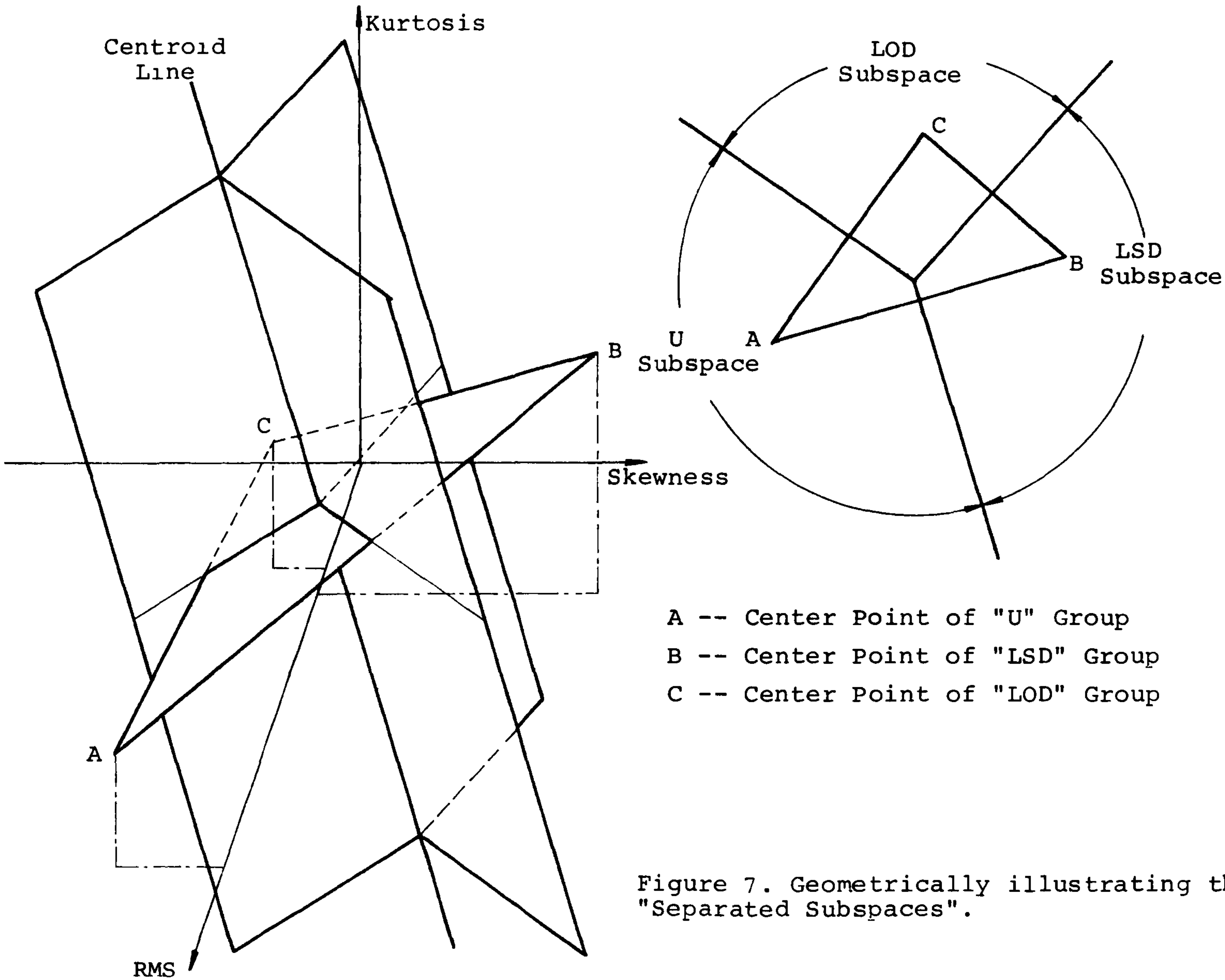

A -- Center Point of "U" Group

B -- Center Point of "LSD" Group

C -- Center Point of "LOD" Group

Figure 7. Geometrically illustrating the "Separated Subspaces".

the three possible alternatives. The classification criteria is to select the region which minimizes the distance to the corresponding center. The best wavelength cutoff is the one for which the most data fit the model. Table (5) shows the results based on the totally separated sphere criteria, while Fig. (6) graphically illustrates the minimized overlapping area idea. The results in Table (5) suggest that the .25 mm cutoff gives the best classification because the number of correct classifications is greatest. Figure (6) also suggests that the .25 mm cutoff is the best to use, because the overlap area is the smallest.

Results with the third model, that using the separated subspaces idea, are given in Tables (6.1-6.3). The distances to all three center points for each specimen are given in each row, with the selection based on the shortest distance. The last columns in Tables (6.1-6.3) indicate a correct or incorrect classification. Based on these results, again the .25 mm cutoff has the greatest discriminating power.

We may conclude that among the three models mentioned above, separated subspaces model is the most suitable one to classify these journal surfaces with regard to their manufacturing method. Also, 0.25 mm wavelength cutoff is proved to have a better power to subdivide surface roughness of journal surfaces.

		Within or out of the predicted range at different wavelength cutoff (mm)		
Type	ID	0.8	0.25	0.08
U	B4	IN	IN	IN
	D4	IN	IN	IN
	E4	IN	IN	IN
	E2	OUT	IN	IN
LSD	C4	OUT	OUT	OUT
	C3	OUT	OUT	OUT
	C1	OUT	OUT	OUT
LOD	F4	IN	IN	OUT
	G4	OUT	IN	OUT
	F3	OUT	OUT	OUT
	G1	OUT	OUT	OUT
	F2	OUT	IN	OUT

Table 5 Results of applying the idea of totally separated sphere range

Wave Length Cutoff (mm)	Group Type	ID	Distances to the three reference center points			Predicted Type	Correct(C) or Wrong (W)
			U	LSD	LOD		
		B4	2.854	8.306	6.826	U	C
	U	D4	5.113	4.954	2.917	LOD	W
		E4	0.499	10.071	8.139	U	C
		E2	6.814	15.956	13.923	U	C
		C4	9.460	4.558	2.752	LOD	W
0.8	LSD	C3	13.287	6.359	9.015	LSD	C
		C1	8.711	2.067	2.163	LSD	C
		F4	7.509	4.443	1.446	LOD	C
		G4	9.337	4.504	2.489	LOD	C
	LOD	F3	7.807	2.881	2.587	LOD	C
		G1	9.812	3.985	5.392	LSD	W
		F2	8.077	7.469	5.402	LOD	C

Table 6.1 Results of "Separated Subspaces" with 0.8 mm wavelength cutoff

Wave Length Cutoff (mm)	Group Type	ID	Distances to the three reference center points			Predicted Type	Correct(C) or Wrong (W)
			U	LSD	LOD		
0.25	U	B4	3.370	9.667	6.987	U	C
		D4	2.423	9.114	5.060	U	C
		E4	1.694	11.550	8.268	U	C
		E2	3.522	12.329	9.136	U	C
	LSD	C4	7.397	6.646	2.327	LOD	W
		C3	9.980	3.864	6.798	LSD	C
		C1	17.457	8.826	13.696	LSD	C
	LOD	F4	6.359	7.155	1.565	LOD	C
		G4	8.879	6.774	2.426	LOD	C
		F3	5.445	7.076	3.182	LOD	C
		G1	7.782	5.997	5.049	LOD	C
		F2	6.793	5.622	1.193	LOD	C

Table 6.2 Results of 'Separated Subspaces' with 0.25 mm wavelength cutoff

Wave Length Cutoff (mm)	Group Type	ID	Distances to the three reference center points: U	LSD	LOD	Predicted Type	Correct (C) or Wrong (W)
0.08	U	B4	3.107	9.721	5.420	U	C
		D4	2.041	10.144	6.646	U	C
		E4	2.332	11.911	9.644	U	C
		E2	2.406	12.451	9.885	U	C
	LSD	C4	6.631	8.944	5.032	LOD	W
		C3	8.716	5.101	1.001	LOD	W
		C1	22.733	13.370	18.620	LSD	C
	LOD	F4	5.941	8.245	4.504	LOD	C
		G4	6.411	7.736	4.427	LOD	C
		F3	9.046	10.815	5.560	LOD	C
		G1	9.959	2.728	3.397	LSD	W
		F2	6.176	8.165	3.299	LOD	C

Table 6.3 Results of "Separated Subspaces" with 0.08 mm wavelength cutoff

V. THE COMPENSATION OF MEASURED SURFACE PROFILE

If we look at the Fig. (2), we may see that when the stylus moves on the profile, the height we really measured at position X_i is Y_i', the locus of the stylus center, which is $Y_i Y_i'$ distant from the real height Y_i. Because of this inevitable measuring error inherent from the geometry of the stylus, particularly the finite radius r, the profile we measured is only the locus of the stylus center, which is different from the true profile, shown in Fig. (2). It is for this reason that it is necessary to compensate for this error so that an actual profile may be drawn.

In general, the best that can be done is to approximately reconstruct the true profile. The following models are those we chose to compensate for some of the error.

As a standard for comparison, the proposed compensation or deconvolution methods are evaluated in terms of their effects on the height sensitive parameters given by Eqs. (5-8) for both mathematically simulated surfaces with known parameters and a measured triangle shaped calibration surface.

STRAIGHT LINE PROFILE MODEL:

Imagine that we have an oblique profile $\overline{PP}$ inclined at angle θ as shown in Fig. (8.a), and consider the tip of the stylus as a ball with radius r. When the stylus measures the oblique line in a direction which is parallel to the datum line, at position X_i the contact point of stylus and surface is C_i, the center of stylus tip is O_i. The measured height at position X_i is Y_i', whereas the true height of the profile at position X_i is Y_i, as shown in Fig. (8a), so there exists an error Y_iY_i' between the measured height and the true height. If we know the slope of the oblique line and the radius of the stylus tip, we can get the actual height at some position X_i by subtracting a distance Y_iY_i' from the measured height at the same position. The distance

$$Y_iY_i' = r\ (\sec\theta - 1)$$

$$= r\ (\sqrt{1 + (dy_i/dx_i)^2} - 1 \qquad (10)$$

where r is the stylus radius, and θ is the tangential angle at contact point C_i.

CONVEX AND CONCAVE PROFILE MODELS:

Referring to Fig. (8b and 8c), imagine that we have a convex or concave profile with a stylus running over it. The contact point of the stylus and profile is C_i, the center of stylus tip at position X_i is O_i, Y_i' is the measured height and Y_i is the true height at the same position X_i. If the radius of stylus tip is r, the radius of curvature of the profile at position X_i is R_i with center at O_i' and the tangential angle θ at contact point C_i are known, we may get the true height Y_i by subtracting the distance Y_iY_i' from the measured height Y_i', which in this instance gives

$$Y_iY_i' = \pm\sqrt{R_i^2 - D_i^2\sin^2\theta}\ \pm D_i\cos\theta - r \qquad (11)$$

where the first term is negative and the second positive if the profile is convex and the opposite signs apply for a concave profile, and

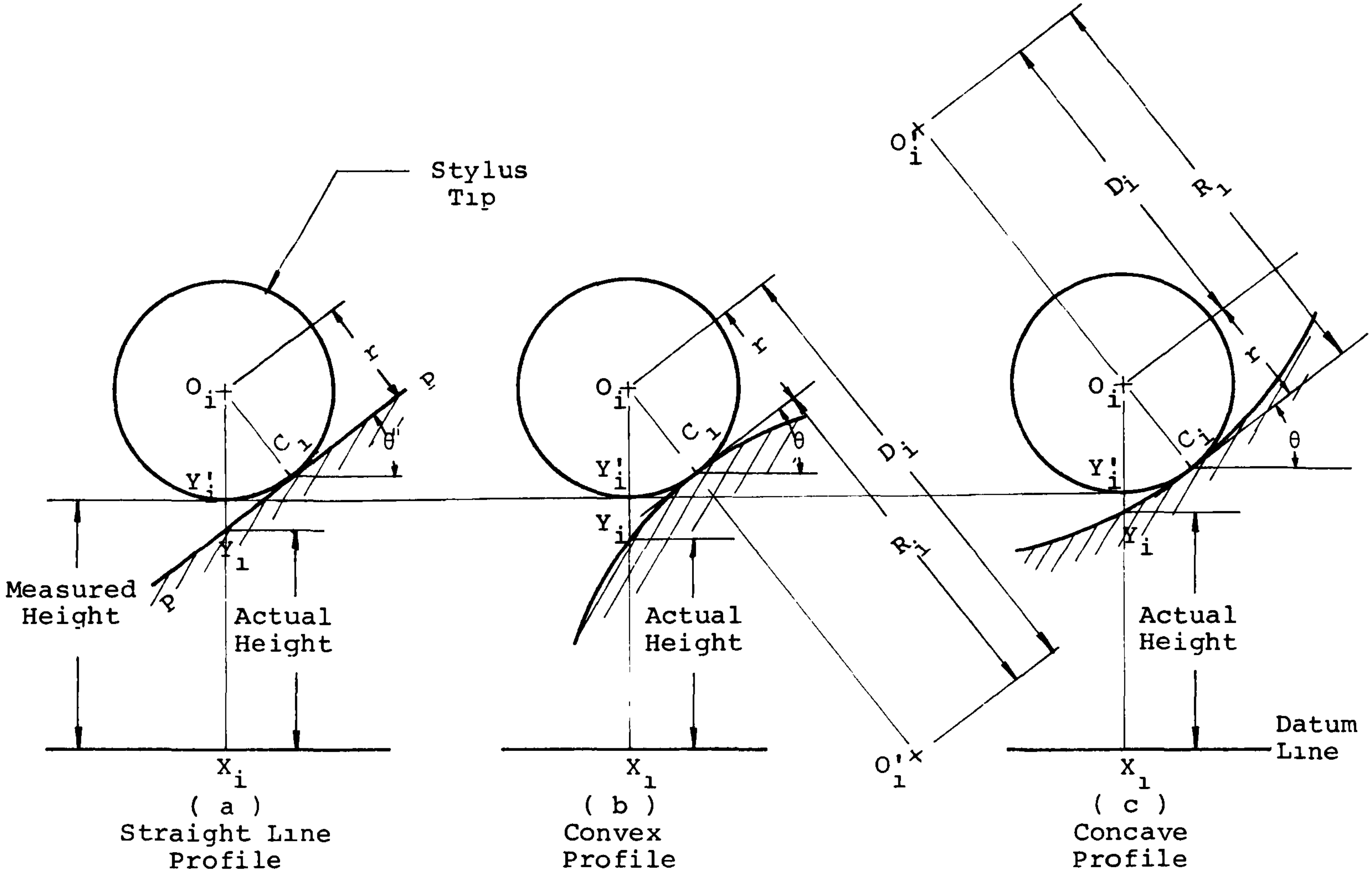

Figure 8. Models of profile contacting with stylus.

$$D_i = r + R_i . \quad (12)$$

The restriction on this solution is

$$R_i^2 \geq \frac{D_i^2}{1 + \frac{1}{(dy_i/dx_i)^2}} \quad (13)$$

The first model, Eq. (10) contains only two variables but the other model, Eq. (11), has more variables that must be determined, in addition to the restriction given by Eq. (13), which can be violated when the angle becomes large or when R becomes smaller than r. Since the first model is simpler to follow and above all, with no limitations on application, we shall continue our discussion on modifying processes based only on Eq. (10).

When applying the straight line model to the measured profile, we need to know the two variables first, the radius of the stylus and the slope of the tangential line at the contact point. The former can be measured directly, but the slope can only be estimated from the profile measurements.

To estimate the slope, dy_i/dx_i, two approaches are used. The first, designated Method I, uses a backward difference approximation to the derivative

$$\frac{dy_i}{dx_i}^{(1)} = \frac{y_i - y_{i-1}}{\Delta x} \quad (14)$$

where the y_i's are the measured profile heights and Δx is the sample interval. Method II amounts to a central difference to estimate the slope, i.e.

$$\frac{dy_i}{dx_i}^{(2)} = \frac{y_{i+1} - y_{i-1}}{2\Delta x} \tag{15}$$

for approximating the slope.

VERIFICATION OF THE PROPOSED METHODS:

To determine how much improvement is possible using the approaches outlined in the previous section, both mathematical simulation and actual profile measurements were used. Fairly simple analytically described functions were used for the profile shapes, viz. a sine wave and a triangle wave. For these shapes, the parameters given by Eqs. (5-8) can be calculated analytically and are:

	Sine	Triangle
R_a	H/π	$H/4$
R_q	$H\sqrt{2}/4$	$H\sqrt{3}/6$
γ_1	0	0
γ_2	1.5	1.8

where H is the peak to valley height. Note that all these parameters are independent of the period, meaning they are only height sensitive. Furthermore, since the skewness and kurtosis are normalized by R_q, they are dimensionless numbers.

The purpose of the mathematical simulation was to be able to eliminate errors introduced in the profile measurements that can be attributed to the manufacturing of reference standards. The analytically defined profile was generated, and the simulation program was designed to provide the resulting motion of the stylus as it traversed this profile. To do this, suppose that the stylus is now at horizontal position X_i, and the profile neighboring to this position is decomposed into discrete points. Assume the vertical position of the stylus center is Y_i", and calculate all the distances between this assumed center point and all the discrete profile points. These distances are compared with the stylus radius; these distances must be all no less than the stylus radius, with at least one distance equal to the stylus radius. We can find the measured height Y_i by iterating the position of the stylus center vertically.

The simulated triangle shaped profile was based on the geometry of a roughness specimen that is used for calibration purposes. This standard is certified to have a roughness $R_a = 3.124 \pm .10$ μm. A profile was made on this standard using the setup shown in Fig. (3) using a $\Delta x = .005$ mm and a stylus radius of 12.7 μm. Figure (9) shows the analog and digitized trace of this sample, and this same data was used for subsequent analysis. Using the data in Fig. (9), the period of the triangle wave was found to be P = 93.133 μm, and the peak to valley height H = 12.497 μm.

The simulation used the 12.7 μm radius and the aforementioned triangle wave characteristics. With the same stylus radius, a sine wave with an amplitude and period the same as the triangle wave was also simulated.

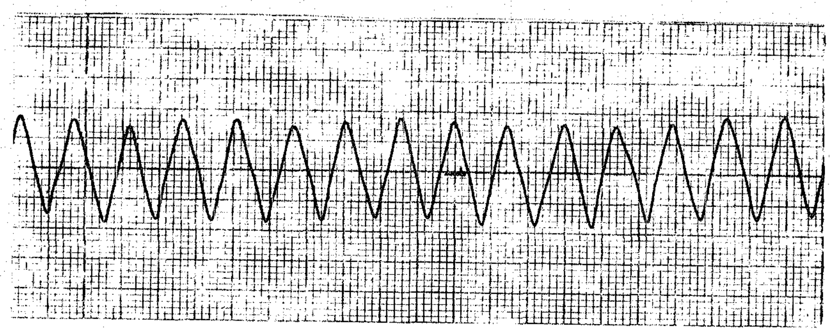

(a)

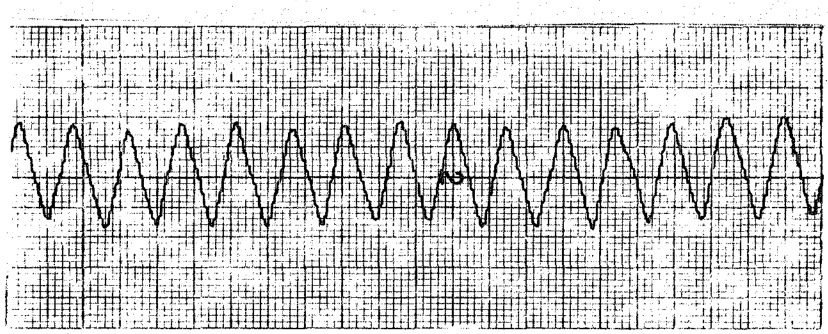

(b)

Figure 9. (a) The continuous profile on channel 1.
(b) The discrete profile on channel 2, of the test specimen.

Table (7) indicates how the theoretical parameters compare with those based on the measurements before compensation to account for stylus radius. Table (8) shows how the height sensitive characteristics are affected by applying Eq. (10) to the simulated measurement and using Method I, Eq. (14), and Method II, Eq. (15), to estimate the profile slope. The errors that correspond to the results in Table (8) are given in Table (9). Table (10), while similar to Table (8), differs from it in that the sine wave profile is simulated, rather than a triangular profile.

There are obvious differences between those parameters calculated from different geometric profiles. The theoretical parameters, which are calculated based on the ideal triangular profile with the specified height and period, are obviously closer to those experimentally measured with stylus. However, there is some difference between the theoretical values and measurements due to the inability to make a perfect standard.

The errors in Table (9) indicate that some improvement in obtaining the height sensitive parameters can be obtained using the methods based on Eqs. (10), (14) and (15). Specifically, for triangle shaped surfaces, the corrections based on Eq. (10) and Eq. (14) gave the best results, with all errors less than .4%. While the overall improvement is not great for an idealized surface like a triangle, the improvement could be greater for real surfaces that are more random.

Ra (μm)	Rq (μm)	γ_1	γ_2
3.014	3.465	-0.026	1.767

Table 7. Parameters of measured triangular wave

	Ra	Rq	γ_1	γ_2
Theoretical	3.124	3.608	0	1.8
Simulated Measurement	3.113	3.592	-0.016	1.776
Corrected using Eqs.(10) and (14)	3.118	3.604	0.033	1.793
Corrected using Eqs.(10) and (15)	3.111	3.594	0.066	1.788

Table 8 Comparison for Simulated Triangle Wave

	Error of Ra	Error of Rq	Error of γ_1	Error of γ_2
Simulated Measurement	-0.011 -0.37%	-0.016 -0.42%	-0.016	-0.024 1.33%
Corrected using Eqs.(10) and (14)	0.006 -0.20%	-0.004 -0.10%	0.033	-0.007 -0.38%
Corrected using Eqs.(10) and (15)	-0.013 -0.49%	-0.004 -0.37%	0.066	-0.012 -0.69%

Table 9 % Error of parameters with theoretical set as basis for simulated triangular wave

	Ra	Rq	r_1	r_2
Theoretical	3.978	4.418	0	1.5
Simulated Measurement	3.911	4.369	-0.185	1.547
Corrected using Eqs.(10) and (14)	4.038	4.481	-0.025	1.482
Corrected using Eqs.(10) and (15)	4.028	4.467	-0.021	1.478

Table 10 Comparison for simulated sine wave.

CONCLUSIONS

Work presented in this report was aimed at trying to find out which statistical parameters estimated from digitized profiles can discriminate between the surface topography of journal surfaces produced by different manufacturing sequences. Results were also presented on different ways to compensate for the errors introduced by having a finite stylus radius on surface profile measurements.

The results presented indicate that:

1. One parameter or pair of parameters can not sufficiently discriminate between different surface topography. Instead, using three parameters, i.e. RMS roughness, skewness, kurtosis, may do this application well.

2. The "Separated Subspaces" in RMS - skewness - kurtosis space is a good model to deal with the classification of the journal surfaces and may be applied to other categorization work. With this criterion, the proper wavelength cutoff for classification analysis is 0.25 mm cutoff.

3. The proposed ways for compensating for the stylus error may correct the measured profile and make it closer to the actual profile. Using both simulated and measured profiles, it was found that improvements can be made using the proposed method, particularly when backward differences are used to estimate the profile slope. Errors for the height sensitive profile parameters of simulated surfaces were less that .4%.

REFERENCES

1. Bellows, Guy, "Surface Integrity of Nontraditional Machining Processes," Proceedings of the International Conference on Surface Technology, SME, May, 1973.

2. Whitehouse, D.J., "Review of Topography of Machine Surface," Proceedings of the International Conference on Surface Technology, SME, May, 1973.

3. El-Helieby, S.O.A., and Rowe, G.W., "Influence of Surface Roughness and Residual Stress on Fatigue Life of Ground Steel Components," Metals Tech., 7:221-5, July, 1980.

4. Briggs, G.A.D., and Briscoe, B.J., "Effect of Surface Topography on the Adhesion of Elastic Solids," App. Phys., 10:2453-66, December 21, 1977.

5. Chow, P.L., and Saibel, E.A., "Roughness Effect in Hydrodynamic Lubrication," Jour. Lubr. Tech., 100:176-9; Discussion 180, April 1978.

6. Kaneta, M., and Cameron, A., "Effects of Asperities in Elasto-hydrodynamic Lubrication." Jour. Lubr. Tech., 102:374-9, July 1980.

7. Purcupile, John C., "The Role of Surface Conditions in Boiling Heat Transfer," Proceedings of the International Conference on Surface Technology, SME, May 1973.

8. Grewal, N.S., and Saxena, S.C., "Effect of Surface Roughness on Heat Transfer from Horizontal Immersed Tubes in a Fluidized Bed," Jour. Heat Transfer, 101:397-403, August 1979.

9. Bannert, K., and Woelk, G.U., "Influence of the Blading Surface Roughness on the Aerodynamic Behavior and Characteristic Anaxial Compressor," Jour. Eng. Power, 102:283-7, April 1980.

10. Haemers, G., Importance of the Surface in Wire Making and Wire Quality," Wire J., 11:134-40, September 1978.

11. Agarwal, R.A., Patki, G.S., and Basu, S.K., "Influence Of Surface Topography on Contact Behaviour of Surfaces," Jour. Inst. Eng. (India) Mech. Eng. Div., V. 59, pt. ME 3, pp. 139-142, November 1978.

12. Osanna, P. Herbert, "Surface Roughness and Size Tolerance," Wear, V. 57, n. 2, December 1979.

13. Shaw, M.C., "The Importance of Solid Surfaces in Science and Engineering," Proceedings of the International Conference on Surface Technology, SME, May 1973.

14. Thomas, T. R., "Surface Roughness Measurement: Alternatives to the Stylus," Int. Metro Conf.: NELEX '78, East Kilbride, Glastow, Scotland, November 28-30, 1978, Issued by Natl. Eng. Lab., East Kilbride, Glasgow, Scotland, 1978, Pap. 4.2, p. 23.

15. American National Standards Institute, B 46.

16. Thomas, T. R., "Characterization of Surface Roughness," Precision Eng., 1981, pp. 97-104.

17. Reason, R. E., "The Bearing Parameters of Surface Topography," Proc. 5th MTDR Conf., Pergamon Press, 1964.

18. Pesante, M., "Determination of Surface Roughness Typology by Means of Amplitude Density Curves," CIRP Ann., 12, 61, 1963.

19. Ehrenreich, M., "The Slope of the Bearing Area as a Measure of Surface Texture," Microtecnic, 1959.

20. Teague, Clayton E., "Uncertainties in Calibrating a Stylus Type Surface Texture Measuring Instrument with an Interferometrically Measured Step," Metrologia, V. 14, N. 1, 1978, pp. 39-44.

21. Whitehouse, D. J., and Vanherk, P., "Survey of Reference Line Used in the Assessment of Surface Texture," CIRP, 21/2, 1972.

22. Shunmugam, M. S., and Radhakrishnan, V., "Selection and Fitting of Reference Line for Surface Profiles, Inst. Mech. Eng. Proc., 190, no. 7:193-201, 1976.

23. Al-Salihi, T., Ph.D. Thesis, University of Birmingham.

24. Wormersley, J. R., and Hopkins, M. R. J., Etats Surface, 135 (1945).

25. Peklenik, J., "Investigation of the Surface Typology," CIRP Ann., 15 381, 1967.

26. DeVries, W. R., "The Surface Topography of Journals," CIRP Annals, Vol. 31/1, 1982.

27. DeVries, W.R., "Documentation for Digital Surface Profile Analysis, the AACIS Program Package," Internal R.P.I. Report, October, 1982.

1 Report No	2 Government Accession No	3 Recipient's Catalog No.
NASA CR-168153		

4 Title and Subtitle
Classification of Journal Surfaces Using Surface Topography Parameters and Software Methods to Compensate for Stylus Geometry

5 Report Date
April 1983

6 Performing Organization Code
779-34-12

7 Author(s)
Cheng-Jih Li, Warren R. DeVries, and Kenneth C Ludema

8 Performing Organization Report No

9 Performing Organization Name and Address
University of Michigan
Ann Arbor, Michigan 48109

10 Work Unit No

11 Contract or Grant No
NCC 3-11

12 Sponsoring Agency Name and Address
U.S. Department of Energy
Office of Vehicle and Engine R&D
Washington, D.C. 20545

13 Type of Report and Period Covered
Contractor Report

14 Sponsoring Agency ~~Code~~ Report No.
DOE/NASA/0011-1

15 Supplementary Notes
Interim report. Prepared under Interagency Agreement DE-AI01-80CS50194. Project Manager L.D. Wedeven, Structures and Mechanical Technologies Division, NASA Lewis Research Center, Cleveland, Ohio 44135.

16 Abstract
This interim report was conducted under NASA Cooperative Agreement NCC 3-11, "Interdisciplinary Collaboration in Tribology-Deconvoluted Surface Profile Measurement with Relevance to Scuffing and Run-In." The initial surface topography of bearing surfaces is a function of the process by which it is made and the material being processed. The appropriate characterization of the surface topography to quantitatively relate it to its functions requires a high degree of finesse. This report concentrates on measurements made with a stylus surface tracer which provides a digitized representation of a surface profile. Parameters are defined to characterize the height (e.g., RMS roughness, skewness, and kurtosis) and length (e.g., autocorrelation) of the surface topography. These are applied to the characterization of crankshaft journals which were manufactured by different grinding and lopping proceedures known to give significant differences in crankshaft bearing life. It was found that three parameters (RMS roughness, skewness, and kurtosis) are necessary to adequately distinguish the character of these surfaces. Every surface specimen has a set of values for these three parameters. They can be regarded as a set coordinate in a space constituted by three characteristics axes. The various journal surfaces can be classified along with the determination of a proper wavelength cutoff (0.25 mm) by using a method of "separated subspaces." The finite radius of the stylus used for profile tracing gives an inherent measurement error as it passes over the fine structure of the surface. A mathematical model is derived to compensate for this error. Using both simulated and measured profiles shows that adjustments can be made to correct the measured profile to make it closer to the actual profile.

17 Key Words (Suggested by Author(s))	18 Distribution Statement
Surface asperities Stylus tracers Surface topography Journal bearings Crankshafts	Unclassified - unlimited STAR Category 37 DOE Category UC-96

19 Security Classif (of this report)	20 Security Classif (of this page)	21 No of pages	22 Price*
Unclassified	Unclassified	51	A04

*For sale by the National Technical Information Service, Springfield, Virginia 22161

End of Document